World Academy of Science, Engineering and Technology
International Journal of Electrical and Computer Engineering
Vol:9, No:6, 2015

Mixed Frequency Excitation of an Electrostatically Actuated Resonator

Abdallah H. Ramini, Alwathiqbellah I. Ibrahim, Mohammad I. Younis

***Abstract*—**We investigate experimentally and theoretically the dynamics of a capacitive resonator under mixed frequency excitation of two AC harmonic signals. The resonator is composed of a proof mass suspended by two cantilever beams. Experimental measurements are conducted using a laser Doppler Vibrometer to reveal the interesting dynamics of the system when subjected to two-source excitation. A nonlinear single-degree-of-freedom model is used for the theoretical investigation. The results reveal combination resonances of additive and subtractive type, which are shown to be promising to increase the bandwidth of the resonator near primary resonance frequency. Our results also demonstrate the ability to shift the combination resonances to much lower or much higher frequency ranges. We also demonstrate the dynamic pull-in instability under mixed frequency excitation.

***Keywords*—**Nonlinear electrostatically actuated resonator.

I. Introduction

THERE has been increasing interest in the complex and distinctive dynamic behavior of resonators, particularly when they are excited by mixed-frequency signals. This interest has been stimulated by their potential use in such fields as communications [1], logic functions [2], [3], and atomic microscopy [4]. For instance, [2] explored use in logic gates. In order to display new logic architectures, they employed mechanical oscillators at different frequencies. Using a single resonator, they built a new algorithm to eradicate wiring by means of condensed Boolean logic. They simultaneously executed their logic gates in efforts to provide a parallel logic circuit in a single mechanical resonator. Mahboob et al. [3] demonstrated parametric coupling between multiple vibrations modes in an electromechanical resonator via a strain inducing piezoelectric pump. This parametric coupling can be useful because it rapidly quenches the vibration of the modes, a reduction that leads to the exchange of the vibration of the modes and of energy. Moreover, their technique helps control the oscillation amplitude and generates high speed. The effect of mixed frequency excitation can be a viable solution in these areas due to mixing frequencies through quadratic electrostatic forces. This method has been found in [1], [4] to realize down converters, mixers, and filters.

Many researchers investigated different ways of mixing signals. In 1977, Hetch [5] analyzed the acousto-optic diffraction with multiple waves at different carrier frequencies using a coupled mode formulation. Later, a three-wave mixing technique was used to find nonlinear index for different transparent material [4]. Nayfeh and Mook [6] derived the analytical expression of multi frequency excitation of a system with a quadratic nonlinearity using straightforward expansion and the method of the multiple scales. Elnagarand and EI-Bassiouny [7] used the method of multiple scales to find the response of three degree of freedom system under multi frequency excitation. They covered different cases of resonance such as harmonic and sub/super harmonic resonances. Later, [8] modeled a multimode mechanical Micro/Nano mechanical resonator with a pulsed parametric pump to convert a mechanical oscillation in a specific mode by transferring the oscillation to a different mode. They modeled the forcing as harmonic actuation and parametric intermodal forces.

There has been considerable attention and interest in understanding the complex MEMS devices behaviors due to mixing wave signals. Levenson [9] used three wave mixing technique to find nonlinear index for different transparent material. Likewise, [10] showed that mixing three waves is a rapid and an effective way to nonlinear refractive indices of glasses. Santos et al. [11] solved the equation of motion to multi-frequency AFM in term of fundamental frequency to measure the attractive and repulsive forces during the oscillation. Erbe and Blick [12] provided a new approach towards realizing Nano machined mechanical mixers of high Eigen frequency. In their work, they choose different driving mechanisms such as surface acoustic waves to ensure operation of the device at room temperature and without any magnetic field.

Notably, [13] fabricated a resonance mixer filter using CMOS-MEMS technology and integrated this mixer filter with amplifiers. He achieved higher gain by selecting low resonance IF with large area electrodes and narrow gaps. Also, [14] successfully demonstrated mixing at RF frequencies over a wide frequency range using integrated micro-resonators on a single-chip with CMOS circuits.

Despite the comprehensive studies on the dynamic behavior of resonators under a single source excitation as well as exploiting nonlinearities for sensing and actuation in MEMS [15]–[19], no research on the dynamic behavior caused by mixed-frequency excitation has been presented so far. Mixed-

A. Ramini is with the King Abdullah University of Science and Technology, Thuwal 23955-6900, Kingdom of Saudi Arabia (phone: +1- 408-454-6307; e-mail: abdallah.ramini@kaust.edu.sa).

A. Ibrahim is with SUNY Binghamton, Binghamton, NY 13850 USA (e-mail: aibrahi4@binghamton.edu).

M. I. Younis was with the Mechanical Eng. Department at SUNY Binghamton, Binghamton, NY 13850 USA. He is now with Physical Sciences and Engineering Division, at King Abdullah University of Science and Technology, Thuwal 23955-6900, Kingdom of Saudi Arabia (e-mail: mohammad.younis@kaust.edu.sa).

frequency excitation in capacitive resonators applications or MEMS devices has not been fully utilized for practical applications.

In this work, we explore the dynamics of an electrostatically biased capacitive accelerometer when excited by two sources of AC loads, where one of the frequencies is constant and the other one is swept over a certain range. When a resonator is excited by these two harmonic sources of frequencies, two new resonances appear when the sum or the difference of these frequencies is equal to the resonance frequency of the device. These are called combination resonances [6], which can be due to the quadratic nonlinearity effect from electrostatic force. Also, another stronger force adds to the previous phenomenon comes from the quadratic form of the voltage source itself, which results in a strong mixing of the AC signals. Here, we exploit additive and subtractive resonances to broaden the bandwidth of the resonator and to generate resonance frequencies at different values of frequency ranges. By fixing one of the excitation frequencies at a small value, the combination resonances become extremely close to the primary resonance, thereby, forming a continuous band of large response at an extended frequency range. We utilize a nonlinear Single-Degree-of-Freedom (SDOF) model to study this behavior theoretically. Finally to compare the measured data with those obtained from the simulations, we conduct several experiments.

II. The Capacitive Resonator

In this section we discuss the details of the experimental and theoretical investigations of the capacitive resonator under study.

A. Device and Experimental Set-Up

The investigated capacitive device is a proof mass suspended by two cantilever beams as shown in Fig. 1. The proof mass represents the upper electrode, which is rectangular in shape of *9 mm* in length, *5.32 mm* in width, and *150 μm* in thickness. Directly underneath the proof mass, a ceramic substrate represents the lower electrode. This ceramic substrate has the same length as the proof mass, but slightly smaller in width = *4.4 mm*. The gap width between the two electrodes is *43.66 μm*. The proof mass vibrates out of the plane with respect to the substrate when excited electrostatically between the two electrodes.

Fig. 1 The tested capacitive sensor

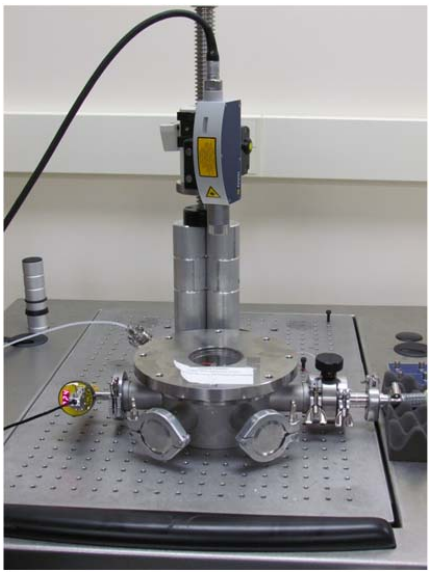

Fig. 2 The LDV pointing at the capacitive resonator inside the vacuum chamber

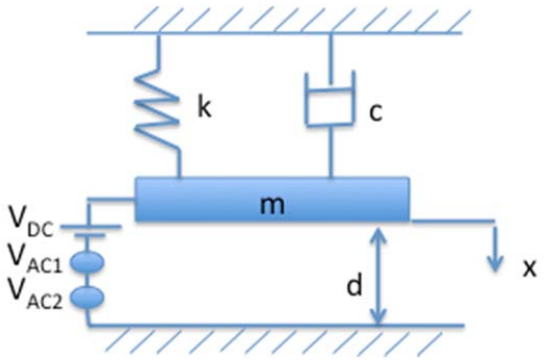

Fig. 3 A SDOF model of the capacitive resonator actuated electrostatically by a DC voltage superimposed to two harmonic AC signals

Fig. 2 presents the experimental set-up used for testing the device. The experimental set-up contains a vacuum chamber, a LabView data acquisition system, AC and DC power sources, and a Laser Doppler Vibrometer (LDV). We place the capacitor inside the vacuum underneath the LDV to measure the deflection of the upper electrode. Then, we reduce the pressure and apply a source of two harmonic AC signals provided by the LabView data acquisition system.

B. Model Formulation

We consider the resonator as a parallel plate capacitor with two rigid plates, where the upper one is movable. We model the resonator as a SDOF model, as schematically illustrated in Fig. 3. The governing equation of motion is expressed as

$$m\ddot{x} + c(x)\dot{x} + kx = \varepsilon_0 \varepsilon_r A \frac{[V_{DC} + V_{AC1}\cos(2\pi f_1 t) + V_{AC2}\cos(2\pi f_2 t)]^2}{2(d-x)^2} \quad (1)$$

We denote the out-of-plane deflection of the proof mass as x. The rest of the parameters are: the mass of the proof mass is

m, the damping coefficient is *c*, the linear effective stiffness of the cantilever beams is *k*, the dielectric constant in the free space is ε_0, the relative permittivity of the gap space medium (air) with respect to the free space is ε_r, the lower electrode area is *A*, the separation gap is *d*, and *t* is time. The electrostatic voltage components are: V_{DC} is DC voltage load and V_{AC1} is the AC voltage load of frequency f_1 and V_{AC2} is the AC voltage load with frequency f_2.

Next, we expand the voltage term, which yields

$$\begin{aligned}&[V_{DC}+V_{AC1}\cos(\Omega_1 t)+V_{AC2}\cos(\Omega_2 t)]^2 = \\ &V_{DC}^2+V_{AC1}^2\cos^2(\Omega_1 t)+V_{AC2}^2\cos^2(\Omega_2 t) \\ &+2V_{DC}V_{AC1}\cos(\Omega_1 t)+2V_{DC}V_{AC2}\cos(\Omega_2 t) \\ &+V_{AC1}V_{AC2}\cos((\Omega_1+\Omega_2)t) \\ &+V_{AC1}V_{AC2}\cos((\Omega_1-\Omega_2)t)\end{aligned} \quad (2)$$

As noticed, combination resonances [6] arise from the expansion of the forcing term when we expand the electrostatic voltage term in (2). Clearly, the last two terms produce combination resonances of additive and subtractive type. In addition, the quadratic nonlinearity of the electrostatic force is likely to produce such summative and subtractive combination resonances.

C. Parameters Extraction

We follow the same characterization process used in [20] to identify the parameters needed to model the device. The parameters *k*, *m*, and *c* in (1) are unknowns based on the previous considerations. Before extracting these parameters, we extract the separation gap by applying a high step-DC-input voltage where the proof mass reaches pull-in. We observed that the static pull-in voltage $V_{DC\ pull\text{-}in} = 161.6\ V$ and the gap $d = 43.66\ \mu m$, as shown in Fig. 4.

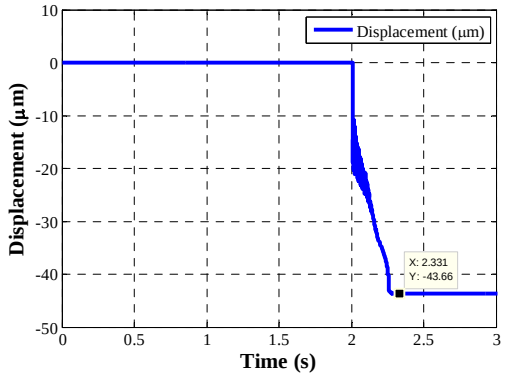

Fig. 4 The response of the capacitive resonator due to a step-DC-input where it reaches the pull-in, the gap $d = 43.66\ \mu m$

To extract the stiffness coefficient *k*, we bias the capacitive structure with V_{DC} input. We ramp the DC voltage at very slow ramping rate to maintain quasi-static loading and measure the static deflection of the proof mass until it reaches the static pull-in. To estimate the stiffness coefficient *k* of the capacitor, we match the experimental deflection with the predicted deflection of the device according to the below equilibrium equation [15]:

$$V_{DC}^2 = 2k/\varepsilon A\left(d^2x - 2dx^2 + x^3\right) \quad (3)$$

Accordingly, we obtain that $k = 330\ N.m^{-1}$. Fig. 5 shows the fitted curve of the simulated deflection of the mass versus the measured displacement.

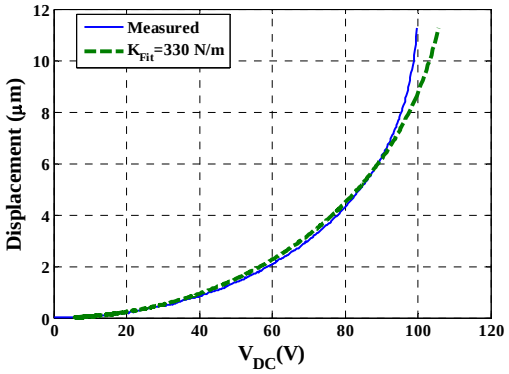

Fig. 5 The simulated deflection versus the measured displacement

To determine the effective mass *m* of the suspended proof mass [20], we excite the capacitive resonator with white noise as shown in Fig. 6. We found that the first symmetric natural frequency f_n, which experimentally occurs at about *193.2 Hz* in Fig. 6. Recalling that the effective mass, $m = k/4\pi^2 f_n^2 = 0.000224\ kg$. To extract the damping coefficient *c*, we curve fit the frequency response to extract the damping ratio, which is found to be $\xi = c/2\sqrt{km} = 0.00027305$.

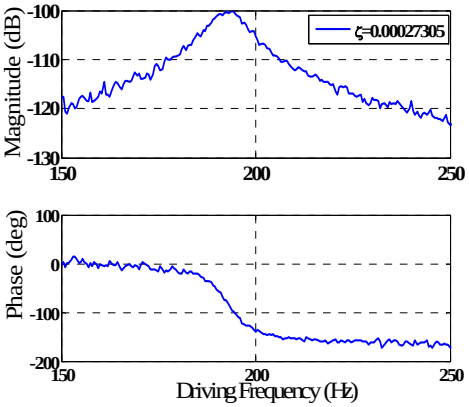

Fig. 6 The experimental frequency curve of the capacitive resonator using white noise

III. Results and Discussion

Next, we investigate the dynamic features arising in the system response when both the frequencies are subtracted ($f_n - f_2$) and when both of the frequencies are summed ($f_n + f_2$). In this context using both forward and backward sweeps, we perform several frequency sweeps while applying a sinusoidal signal at a fixed frequency (f_2) while sweeping the other frequency (f_1). We sweep the frequency slowly, to guarantee

the steady-state condition at the end of each step. The purpose is to analyze the device response behavior in the neighborhoods of (f_n–f_2) and ($f_n + f_2$), while keeping the values of the electrodynamic voltages V_{AC1} and V_{AC2} constants. We report the experimental forward frequency sweep at $V_{DC} = 4\ V$, $V_{AC1} = 2\ V$ and $V_{AC2} = 8\ V$ in Fig. 7 (a). As a result, typical resonant behavior around *193.2 Hz* is noticed. In addition, we can notice the small peaks at the combination frequencies coming from the subtraction/addition of ($f_2 = 1\ Hz$) from/with the fundamental resonance frequency. Fig. 7 (b) shows a zoom on the experimental and the theoretical sweeps of the subtractive combination frequency at *192.2 Hz*. The theoretical sweeps are generated using long time integrations. These observations indicate that these frequencies follow the qualitative behavior of the fundamental natural frequency. For example, if there is a softening behavior, the combination frequencies have a softening behavior. Also, this applies on the hardening and dynamic pull-in behaviors [16].

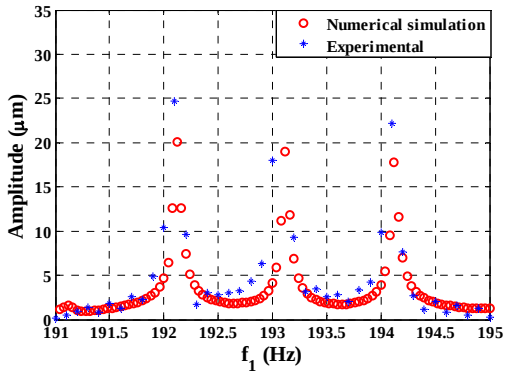

(a)

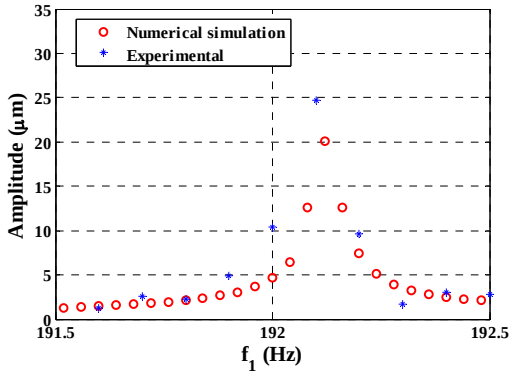

(b)

Fig. 7 (a) The experimental and numerical simulation of frequency response curves due to $V_{DC} = 4\ V$, $V_{AC1} = 2\ V$, $f_2 = 1\ Hz$ and the damping ratio $\xi = 0.00165$. (b) Enlarged view of the subtractive type resonance at the combination resonance frequency ($f_{sub} = f_n - f_2$)

To increase the amplitude of the combination frequencies at ($f_n - f_2$) and ($f_n + f_2$), we increase the amplitude of V_{AC2}. In addition, we use a smaller frequency ($f_2 = 500\ mHz$). Similarly, we report the experimental frequency sweeps due to at $V_{DC} = 4\ V$, $V_{AC1} = 2\ V$ and different values of V_{AC2} in Fig. 8. The results indicate that the response levels (floors) between the combination frequencies and the primary resonance increase to magnitudes close to that of the primary resonance. At the same time, there is a very small change in the amplitude of the primary resonance due to V_{AC2}. We can notice that the level between the primary resonance and the combination frequencies has increased to a high measureable level around *7 µm*. The mixed frequency excitation increases the bandwidth of the resonator. In other words, mixed-frequency excitation may effectively excite resonators with extended ranges of frequencies, and meanwhile avoid the limited frequency ranges of narrow sharp responses that undesirably affect the performance of resonators. If we apply more V_{AC2} voltage, we can increase this level higher to utilize this as a wide band pass filter. It is also clear that the amplitude of the combination frequency is associated the voltage with the fixed frequency of V_{AC2}. If we increase V_{AC2}, the amplitude increases.

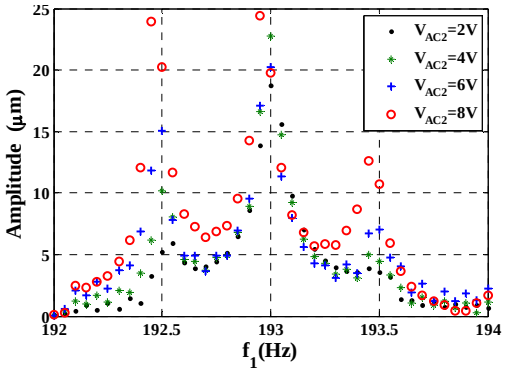

Fig. 8 The experimental frequency response curves due to different values of V_{AC2}. The rest of the parameters are $V_{DC} = 4\ V$, $V_{AC1} = 2\ V$ and $f_2 = 500\ mHz$

To shift the primary resonance to smaller or larger frequency ranges, we apply a harmonic signal of fixed amplitude and fixed frequency at $f_2 = 50\ Hz$ and similarly extract the frequency response curves of the capacitive resonator. In Fig. 9, frequency response curves show resonances activated at *142.2 Hz* and *242.2 Hz* due to $V_{DC} = 4\ V$, $V_{AC1} = 2\ V$, $V_{AC2} = 2\ V$ and $f_2 = 50\ Hz$. These results are interesting since they demonstrate the possibility of shifting the resonance of very stiff MEMS structures to lower values, which can be used in low frequency range applications, for example in energy harvesting.

Next, we investigate the mixed frequency excitation to trigger the dynamic pull-in at the primary resonance. Dynamic pull-in phenomenon is system instability that can be triggered due to the AC harmonic loading [15]. Also, we call the instability range of frequency where pull-in occurs "pull-in band" [21], [22]. To illustrate this, we first set the fixed frequency source at zero ($V_{AC2} = 0\ V$ *and* $f_2 = 0\ Hz$) to show the effect of the sweeping frequency alone without the effect of other sources. In Fig. 10, we show the pull-in bands caused by the forward and backward sweeping of the frequency of the electrostatic voltage.

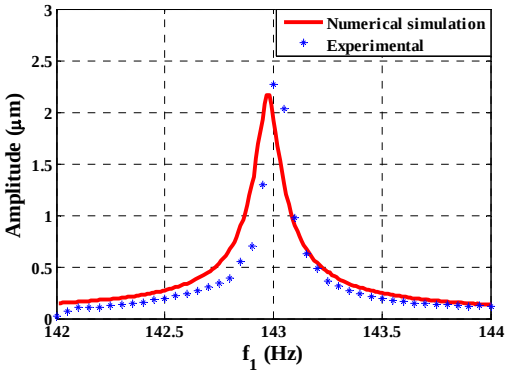

(a)

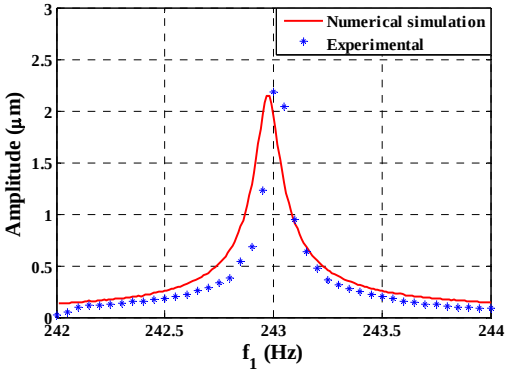

(b)

Fig. 9 The experimental and simulated frequency response curves due to $V_{DC} = 4\ V$, $V_{AC1} = 2\ V$, $V_{AC2} = 2\ V$ and f_2=50 *Hz*. The extracted damping ratio is ξ=0.0002. (a) The subtractive combination frequency ($f_{sub} = f_n - f_2$). (b) The additive combination frequency ($f_{sub} = f_n + f_2$)

Following, we study the effect of the mixed frequency excitation on the pull-in band by using a signal of frequency ($f_2 = 2\ Hz$). Similarly, we extract the frequency response curves with pull-in bands in Fig. 11 where we show results for the forward and the backward sweeps. In these figures, we report the experimental forward and backward frequency sweeps at $V_{DC} = 5\ V$, $V_{AC1} = 4\ V$ and V_{AC2}=8 *V*. As a result, two more pull-in bands generated from mixing the second harmonic signal source with the swept source similar to the previous experimental data but here, it transfers the nonlinear behavior to these combination resonances. This observation indicates and proves that these combination frequencies follow qualitatively the behavior of the primary resonance. The ability to generate multiple pull-in bands of the device is a feature that can benefit MEMS switches applications. Also we note that the size of these combination pull-in bands is smaller than the size of pull-in band in the primary resonance.

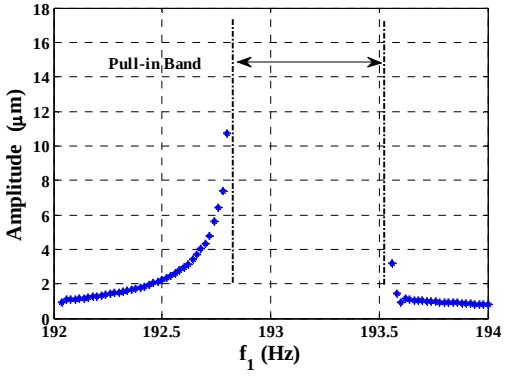

(a)

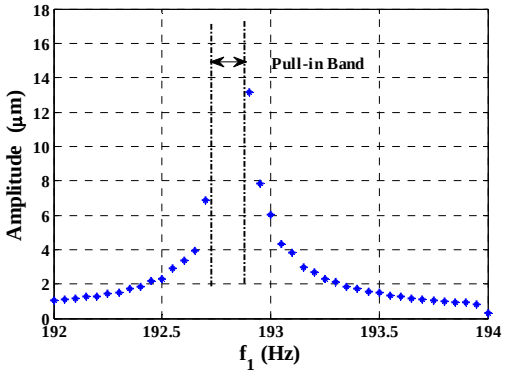

(b)

Fig. 10 The experimental frequency response curve due to $V_{DC} = 5\ V$, $V_{AC1} = 4\ V$, $V_{AC2} = 0\ V$ *and* f_2=0 *Hz* (a) The forward sweep. (b) The backward sweep

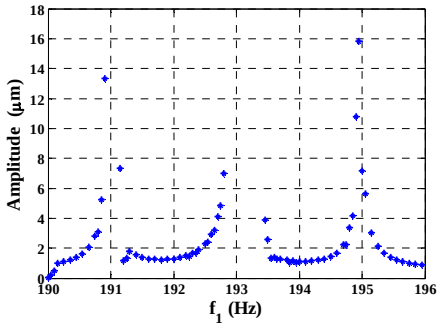

(a)

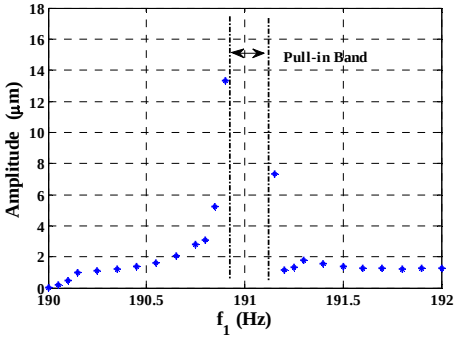

(b)

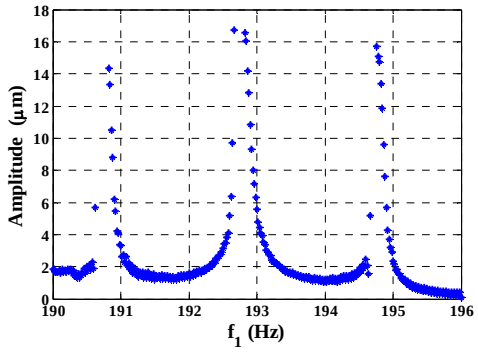

(c)

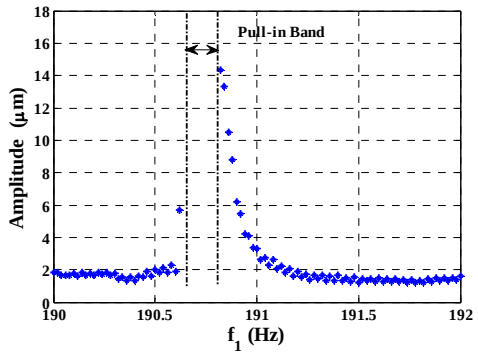

(d)

Fig. 11 The measured frequency response curve due to $V_{DC} = 5\ V$, $V_{AC1} = 4\ V$, $V_{AC2} = 8\ V$ and $f_2 = 2\ Hz$. (a) The forward frequency sweep. (b) Zoom on the subtractive combination frequency ($f_{sub} = f_n - f_2$). (c) The backward frequency sweep. (d) Zoom on the subtractive combination frequency ($f_{sub} = f_n - f_2$)

IV. Summary and Conclusions

We studied an electrostatically actuated capacitive resonator using mixed frequency of two harmonic AC signals to illustrate the dynamic features arising in the system. We experimentally tested the capacitive resonator in the neighborhoods of the resonance frequency emerging from two harmonic sources when the sum or difference of these frequencies is equal to the natural resonance frequency of this resonator. Also, we simulated the frequency responses curves using long time integration of a single degree of freedom system. Thus, we were able to produce multiple resonances with desired amplitude and desired frequencies by carefully choosing the input voltage and input frequency. This method could offer a novel solution in band pass filters by applying many small frequencies to create the desired bandwidths. As shown in this paper, we decreased the biased constant frequency to *500 mHz* and hence, a shape of broader bandwidth started to develop. The other intriguing feature is that generating a combination resonance frequency at low frequency range can help increase the amount of energy harvested from the environment using MEMS harvesters that have very high resonance frequencies. Also, by applying large exciting frequency close to the predicated resonance, we can use this method to measure the resonance frequencies of MEMS and NEMS devices that have very high resonances and very stiff structures, due to the limitations in frequency ranges of some optical measurement devices. Finally, this method could be used in MEMS switches to transfer the pull-in band to small ranges of frequencies far from the primary resonance frequencies of MEMS mass switches and acceleration switches [16], [22].

References

[1] A. C. Wong and C. C Nguyen, "Micromechanical Mixer-Filters ("Mixlers")," *J. of Microelectromechanical Sys.*, vol. 13, no. 1, pp. 100-112, Feb. 2004.

[2] I. Mahboob, E. Flurin, K. Nishiguchi, A. Fujiwara, and H. Yamaguchi, "Interconnect-Free Parallel Logic Circuits in a Single Mechanical Resonator," *Nature Communications 2*, Article number: 198 doi:10.1038/ncomms1201, Feb. 2011.

[3] I. Mahboob, V. Nier, K. Nishiguchi, K., A. Fujiwara, and H. Yamaguchi, "Multi-Mode Parametric Coupling in an Electromechanical Resonator," *Appl. Phys. Lett.*, vol. 103, 153105, 2013.

[4] R. Garcia and E. T. Herruzo, "The Emergence of Multifrequency Force Microscopy," *Nature nanotechnology*, vol. 7, no. 4, pp. 217-226, 2012.

[5] D. Hecht, "Multifrequency Acoustooptic Diffraction," *IEEE TRANS. ON Sonics and Ultrasonics*, vol. SU-24, no. 1, 1977.

[6] A. H. Nayfeh and D. T. Mook, *Nonlinear Oscillations.* New York: Wiley-Interscience, 1979, pp. 183–188.

[7] A. M. Elnagarand and A. F. EI-Bassiouny, "Response of Self-Excited Three-Degree-of-Freedom Systems to Multifrequency Excitations," *Inter. J. of Theoretical Phys.*, vol. 31, no. 8, 1992.

[8] H. Yamaguchi, H. Okamoto, and I. Mahboob, "Coherent Control of Micro/Nanomechanical Oscillation Using Parametric Mode Mixing," *Appl. Phys. Express*, vol. 5, 014001, 2012.

[9] Marc D. Levenson, "Feasibility of Measuring the Nonlinear Index of Refraction by Third-Order Frequency Mixing," *IEEE J. of Quantum Electronics*, vol. 10, no. 2, pp. 110-115, Feb. 1974.

[10] R. Adair, L. L. Chase and S. A. Payne, "Nonlinear Refractive-Index Measurements of Glasses Using Three-Wave Frequency Mixing," *JOSA B*, vol. 4, no. 6, pp. 875-881, 1987.

[11] S. Santos, K. R. Gadelrab, V. Barcons, J. Font, M. Stefancich, and M. Chiesa, "The Additive Effect of Harmonics on Conservative and Dissipative Interactions," *J. of Appl. Phys.*, vol. 112, no. 12, 124901, 2012.

[12] A. Erbe and R. H. Blick, "Silicon-on-Insulator Based Nanoresonators for Mechanical Mixing at Radio Frequencies," *IEEE Trans. On Ultrasonics, Ferroelectrics and Frequency Control*, vol. 49, no. 8, pp. 1114-1117, Aug, 2002.

[13] G. K. Fedder, "CMOS-MEMS Resonant Mixer-Filters," *IEEE International Electron Devices Meeting, Washington, DC*, Dec. 2005, pp. 274-277.

[14] F. Chen, J. Brotz, U. Arslan, C. C. Lo, T. Mukherjee, and G. K. Fedder, "CMOS-MEMS Resonant RF Mixer-Filters," *Tech. Dig. 18th IEEE Int. Conf. on Micro Electro Mechanical Systems (MEMS'05)*, Jan. 2005, pp. 24-7.

[15] M. I. Younis, *MEMS Linear and Nonlinear Statics and Dynamics*. Springer, 2011, Ch. 7.

[16] J. F. Roads, S. W. Shaw. K. L. Turner, "Nonlinear Dynamics and Its Applications in Micro- and Nanoresonators," *J. of Dyn. Systems Measurement, and Control*, vol. 132, 2010, p. 14.

[17] I. Kozinsky, H. W. C. Postma, O. Kogan, A. Husain, and M. L. Roukes, "Basins of attraction of a nonlinear nanomechanical resonator," *Physical Review Lett.*, vol. 99, no. 20, 2007, 207201.

[18] C. Stambaugh and H. B. Chan, "Noise-activated switching in a driven nonlinear micromechanical oscillator," *Physical Review Lett.*, vol. 73, no. 17, 2006, pp. 172-302.

[19] V. Kumar, J. William Boley, Y. Yang, G. T.-C. Chiu, and J. F. Rhoads, "Modeling, Analysis, and Experimental Validation of a Bifurcation-Based Microsensor," *J. of Microelectromechanical Sys.*, vol. 21, no. 3, 2012, pp. 549-558.

[20] A. H. Ramini, M. I. Younis, Q. Sue, "A Low-G Electrostatically Actuated Resonant Switch," *Smart Mater. Struct.*, vol. 22, no. 22, 025006(13pp), Dec. 2013.

[21] F. Alsaleem, M. I. Younis, and L. Ruzziconi, "An Experimental and Theoretical Investigation of Dynamic Pull-in in MEMS Resonators Actuated Electrostatically," *J. of Microelectromechanical Sys.*, vol. 19, no. 4, 2010, pp. 794 - 806.
[22] F. Alsaleem, M. I. Younis, and H. Ouakad, "On the Nonlinear Resonances and Dynamic Pull-in of Electrostatically Actuated Resonators," *J. of Micromechanics and Microengineering*, vol. 19, 2009, 045013.

Abdallah Ramini (M'15) was born in Amman, Jordan, in 1981. He received the Bachelor and Master's degrees from Jordan University of Science and Technology in Mechatronics Engineering, Jordan in 2004 and 2007, respectively; and the Ph.D. degree in Mechanical Engineering from Binghamton State University of New York in 2012, with a focus on the static and dynamic behaviors of MEMS devices and structures under shock. From 2012 to 2013, he was with Binghamton State University of New York as a Post-Doctoral Fellow working on dynamical integrity of MEMS resonators. Since 2013, he was King Abdullah University of Science and Technology in Saudi Arabia as Post-Doctoral Fellow. Currently, he is performing his research activity with MEMS and NEMS Characterization and Motion Laboratory. His research focuses on MEMS resonant and actuator applications. Dr. Ramini is a member of the American Society of Mechanical Engineers ASME.